Available online at www.sciencedirect.com

ScienceDirect

Procedia Materials Science 3 (2014) 1971 – 1976

Procedia Materials Science

www.elsevier.com/locate/procedia

20th European Conference on Fracture (ECF20)

# Dynamic nonlinear crack growth at interfaces in multi-layered materials

Mauro Corrado[a,*], Marco Paggi[b]

[a]*Department of Structural, Geotechnical and Building Engineering, Politecnico di Torino, C.so Duca degli Abruzzi 24, 10129 Torino, Italy*
[b]*IMT Institute for Advanced Studies Lucca, Piazza San Francesco 19, 55100 Lucca, Italy*

**Abstract**

Finite thickness interfaces, such as structural adhesives, are often simplified from the modelling point of view by introducing ideal cohesive zone models that do not take into account the finite thickness properties in the evaluation of the interface stiffness and inertia. In the present work, the nonlinear dynamic response of those layered systems is numerically investigated according to the finite element method. The weak form of the dynamic equilibrium is written by including not only the contribution of cohesive interfaces related to the virtual work exerted by the cohesive tractions for the corresponding relative displacements, but also considering the work done by the dynamic forces of the finite thickness interfaces resulting from their inertia properties. A fully implicit solution scheme both in space and in time is exploited and the numerical results for the double cantilever beam test show that the role of finite thickness properties is remarkable as far as the crack growth kinetics and the dynamic strength increase factor are concerned.


Selection and peer-review under responsibility of the Norwegian University of Science and Technology (NTNU), Department of Structural Engineering

*Keywords:* Multi-layered materials; finite-thickness interfaces; cohesive zone model; dynamic fracture; FEM

## 1. Introduction

There are several systems in nature and technology where different materials are separated by interfaces with a not negligible thickness. Often this property is neglected in numerical simulations and the interface is simplified as a geometrical entity with zero-thickness (a line in 2D or a surface in 3D) where displacement discontinuities may take place. The transmitted tractions are on the other hand continuous across the interface due to equilibrium considerations and are usually nonlinear functions of the relative opening and sliding displacements via the so-called *cohesive zone models* (CZMs) (Elices et al. (2002)).

However, the thickness of interfaces is not always negligible and it has been proven to have a significant effect on the overall quasi-static properties of heterogeneous materials. In spite of that, the study of these systems is still partially unchallenged. The complexity relies in the difficulty of modeling nonlinear phenomena taking place within a

* Corresponding author. Tel.: +39-011-090-4858 ; fax: +39-011-090-4899.
*E-mail address:* mauro.corrado@polito.it


Selection and peer-review under responsibility of the Norwegian University of Science and Technology (NTNU), Department of Structural Engineering
doi:10.1016/j.mspro.2014.06.317

very narrow zone, often at least one order of magnitude smaller than the joined material regions. In Paggi and Wriggers (2011a,b), the interface region was treated as a continuum with a physically-defined finite thickness. A damage mechanics formulation was introduced to model its nonlinear behavior under tension, shear and their combination. The non locality of damage was also properly taken into account by using a damage variable dependent on the relative displacements evaluated at the boundary of the finite thickness region, which are by definition nonlocal quantities since they are the integral of the strain field inside the interfacial zone. Inelastic stress-relative displacement relations were determined and their nonlinear shape was dependent on the evolution of damage. To simplify the computational burn, an equivalence between the finite thickness interface with damage mechanics and a zero thickness interface whose mechanical response is ruled by a novel type of CZM was also put forward in Paggi and Wriggers (2011a,b). This modeling strategy was particularly effective for interpreting numerical studies aiming at extracting CZMs from molecular dynamics and atomistic simulations (Spearot et al. (2004); Yamakov et al. (2006); Wolf et al. (2005)) on systems with finite thickness regions. Moreover, applications to polycrystalline materials with standard or hierarchical microstructures were proposed in Paggi and Wriggers (2011b, 2012).

Regarding the dynamic behavior of finite thickness interfaces, much less contributions are available in the literature. The concept of structural interface introduced by Bigoni and Movchan (2002) was pioneeringly proposed to model a real structure possessing a finite thickness which joins continuous materials. With special regard to fiber reinforced interfaces leading to bridged cracks, Bertoldi et al. (2007a,b) have shown that the introduction of structural interfaces involves a nonlocal mechanical behavior. Independent results supporting the findings by Bertoldi et al. (2007a,b) have been presented by Tang et al. (2005), with reference to the problem of adhesion, and by Sumigawa et al. (2008), who provided experimental observation of imperfect interfaces consisting of nano-springs. Bigoni and Movchan (2002) and Brun et al. (2010) noticed that a thick interface possesses a mass that can strongly influence dynamic characteristics, both for structural interfaces and for interfaces made up of inertial elastic layers.

In the present study, a progress on the research on the behavior of finite thickness interfaces is made with regard to their dynamic regime.

## 2. Equations of motion, cohesive zone model and finite element approximation

Dynamic equilibrium of a solid body with volume $V$, external boundary $\partial V$ and internal cohesive cracks $S$ is provided by the principle of virtual work:

$$\int_V (\nabla \boldsymbol{\eta})^{\mathrm{T}} \boldsymbol{\sigma} \mathrm{d}V - \int_V \boldsymbol{\eta}^{\mathrm{T}} \rho_v \ddot{\boldsymbol{\eta}} \mathrm{d}V - \int_{\partial V} \boldsymbol{\eta}^{\mathrm{T}} \mathbf{f} \, \mathrm{d}S - \int_S \mathbf{g}^{\mathrm{T}} \mathbf{t} \, \mathrm{d}S - \int_S \boldsymbol{\eta}^{\mathrm{T}} \rho \, t \, \ddot{\boldsymbol{\eta}} \mathrm{d}S = 0 \tag{1}$$

where the first term is the internal virtual work of deformation given by the tensorial product between stresses and strains, the second term is the work by dynamic forces ($\rho_V$ is the mass density of the bonded layers and $\ddot{\boldsymbol{\eta}}$ are the accelerations), the third term is the virtual work of the tractions $\mathbf{f}$ acting on the boundaries of the body $\partial V$, the forth term represents the virtual work of the interface normal and tangential cohesive tractions $\mathbf{t} = (\tau, \sigma)^{\mathrm{T}}$ for the corresponding relative sliding and opening displacements $\mathbf{g} = (g_{\mathrm{T}}, g_{\mathrm{N}})^{\mathrm{T}}$ at cohesive interfaces $S$, and the last term is the finite thickness interface contribution to the work by dynamic forces ($\rho$ and $t$ are, respectively, the mass density and the thickness of the adhesive).

To simulate the phenomenon of layer debonding in laminated composites by taking into account the finite thickness properties of the adhesive, we introduce here a CZM whose shape is characterized by a linear ascending branch followed by an exponential softening. The slope of the linear branch, $K$, can be estimated by the ratio between the Young modulus of the adhesive, $E_{\mathrm{adh}}$, and the adhesive thickness, $t_{\mathrm{adh}}$, i.e., $K = E_{\mathrm{adh}}/t_{\mathrm{adh}}$. This is usually put forward in the literature to estimate the properties of an adhesive layer modeled as a bed of linear springs (Camanho and Davila (2002); Li et al. (2005)). In the present model, the selection of the initial stiffness of the CZM depending on the adhesive properties can be made by varying the internal parameter $l_0$, which defines the opening and sliding displacements corresponding to the peak CZM tractions before the onset of exponential softening. The resulting

expression for the normal cohesive tractions is:

$$\sigma = \begin{cases} \sigma_{\max} \exp\left(\dfrac{-l_0 - |g_T|}{R}\right)\dfrac{g_N}{l_0}, & \text{if} \quad \dfrac{g_N}{R} < \dfrac{l_0}{R} \\ \sigma_{\max} \exp\left(\dfrac{-g_N - |g_T|}{R}\right), & \text{if} \quad \dfrac{l_0}{R} \leq \dfrac{g_N}{R} < \dfrac{g_{Nc}}{R} \\ 0, & \text{if} \quad \dfrac{g_N}{R} \geq \dfrac{g_{Nc}}{R} \end{cases} \tag{2}$$

The other parameters entering the formulation are the critical opening displacement, $g_{Nc}$, corresponding to complete debonding in pure Mode I loading, and the root mean square of the heights of the microscopically rough crack profile, $R$.

Due to vibrations induced by stress waves traveling through the body in the transient regime, partial or complete crack closure with contact may frequently take place (Carpinteri et al. (2008)). In this instance, we consider a linear elastic unloading and reloading from the point of the CZM corresponding to the maximum experienced relative displacement to zero, and viceversa. In case of crack contact, a penalty formulation is used, with a penalty parameter $pn$ equal to the same stiffness $K$ as in tension.

Upon discretization of Eq.(1) with finite elements, the governing equations in matrix form become:

$$\boldsymbol{M}\ddot{\boldsymbol{\eta}} + \boldsymbol{F}^{\text{int}} = \boldsymbol{F}^{\text{ext}}, \tag{3}$$

where $\boldsymbol{M}$ is a lumped mass matrix, $\boldsymbol{F}^{\text{int}}$ is the internal force array arising from the current state of stress (equal to the stiffness matrix times the vector of nodal displacements) and $\boldsymbol{F}^{\text{ext}}$ is the external force array including surface tractions acting on the boundary $\partial V$ and on the cohesive interfaces $S$.

Hence, cohesive interfaces contribute to Eq.(3) for all of the three terms. By using interface elements to discretize cohesive interfaces as in Paggi and Wriggers (2011b, 2012) and considering an implicit solution scheme, their internal force array contribution is given by the tangent stiffness matrix multiplied by the nodal displacement vector. In particular, a 4-nodes linear interface element has been implemented as a new user element in the finite element programme FEAP. All the details of the implementation can be found in Paggi and Wriggers (2011b, 2012).

Regarding the mass matrix of the interface element, which, to the best of the authors' knowledge, is always neglected in the literature, is given by a lumped approximation:

$$\mathbf{M} = \frac{\rho t l}{4}\mathbf{I} \tag{4}$$

where $\mathbf{I}$ is a $8 \times 8$ identity matrix, $\rho$ is the mass density of the adhesive, $t$ is the adhesive thickness and $l$ is the element length.

## 3. Numerical investigation

As a test problem, let us consider a double cantilever beam (DCB) test, which is frequently used in experiments to assess the bonding strength of adhesives. The sketch of the test and the dimensions are shown in Fig.1. The mechanical properties of the linear elastic laminae are those of Aluminum, $E_{\text{Al}} = 70$ GPa, $\nu_{\text{Al}} = 0.3$ and $\rho_{\text{Al}} = 2700$ kg/m$^3$. The parameters of the adhesive (CZM) are: Young modulus $E_{\text{adh}} = 0.42$ GPa, tensile strength $\sigma_{\text{peak}} = 8.5$ MPa, critical Mode I debonding length $g_{Nc} = 0.3$ mm, fracture energy $G_F = 600$ N/m. Parametric analyses will be performed by varying the line-loading displacement velocity, $v$, the adhesive thickness, $t_{\text{adh}}$, and the adhesive mass density, $\rho$.

A plane stress FE model is considered with 4-nodes isoparametric finite elements for the discretization of the continuum. At least 10 elements are employed through each layer thickness and the finite element size is $75 \times 100$ $\mu$m to resolve with the necessary accuracy the cohesive tractions in the process zone, which has a size approximately equal to 3 mm. The computation is performed under the assumption of small displacements. At each time step, the solution of the equilibrium equations is achieved by the Newton-Raphson method. Integration in time is performed by a Newmark constant-average-acceleration scheme ($\beta = 0.5, \gamma = 0.25$) and a time step of $t = 0.5$ $\mu$s, which is less than the time that a longitudinal wave would need to cross the process zone size, which is about 2 $\mu$s.

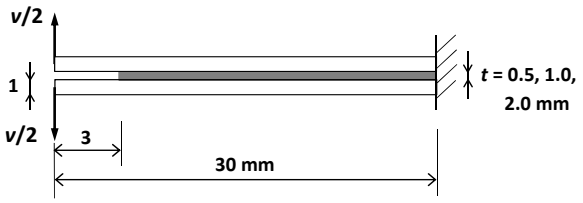


Fig. 1. Sketch of the double cantilever beam test.

The numerical simulations are performed by imposing a load-line displacement at the beam tip with a prescribed velocity $v$. However, instead of imposing the prescribed constant velocity from the very beginning of the simulation, a ramp function is considered to provide a smooth transition from the initial configuration to the steady-state velocity. The introduction of this ramp function was found to be essential to avoid spurious vibrations in the layered beam, without the need of introducing any damping in the model.

The first set of numerical results concerns the effect of the load-line displacement velocity on the mechanical response as compared to the quasi-static case. For this test we select $t = 0.5$ mm, $\rho = 2700$ kg/m$^3$ and different load-line displacement velocities, $v = 5$, 10, 15 or 20 m/s. The line-load, given by the reaction force under the point of application of the displacement, is plotted vs. the load-line displacement in Fig.2(a). By increasing the velocity $v$, an increase in the peak load due to dynamic effects is clearly observed. This is the result of the interplay between the CZM properties and the inertia forces and it not related to rate-dependent parameters. By plotting the line-load vs. the fictitious crack-tip position, Fig.2(b), we also notice that the process zone size at the peak load shrinks by increasing the line-loading velocity. The fictitious crack-tip position is set at the point along the interface where the peak cohesive traction takes place. Finally, the crack-tip velocity is an increasing function of the line-displacement velocity $v$, as shown in Fig.2(c). In particular, it is important to note that the crack velocity is highly dependent on the fictitious crack-tip position, with a maximum followed by a descending branch down to an asymptotic value for very long cracks. The dynamic increase factor, DIF, is computed as the ratio between the peak load in the dynamic case and the peak load from the quasi-static simulation and it is plotted in Fig.2(d) vs. $v$. Dynamic effects lead nearly to 40% of peak load increase for the highest velocity tested.

These results show that the dynamic properties of the system can provide an explanation to the observed strength increase as compared to the quasi-static regime. However, for very high strain rates, a yet unexplained dramatic increase in strength is often found in experiments (Malvar and Ross (1998); Caveran et al. (2013)). Since pure inertia effects are not enough to explain this phenomenon, rate-dependent CZMs are employed, where the fracture energy is empirically related to the crack-tip velocity (Zhou et al. (2008)) or to the crack opening rate (Corigliano et al. (2006)). In the present problem where the crack path is defined a priori without the occurrence of crack branching, the application of those rate-dependent models would be easy to implement.

The effect of the adhesive thickness is investigated in Fig.3 for an adhesive with $\rho = 2700$ kg/m$^3$. A change of adhesive thickness results into a modification of the interface element stiffness $K$. In particular, since $K = E_{\rm adh}/t_{\rm adh}$, thicker adhesives are more compliant than thinner ones. We explore thicknesses of 0.5 mm, 1.0 mm and 2.0 mm. The peak cohesive tractions and the fracture energy of the adhesive are kept the same in all the simulations. Since a change of adhesive thickness influences the linear branch of the CZM, thickness effects are already observed in the quasi-static regime, see the load vs. the load-line displacement diagram in Fig.3(a). Considering $t = 0.5$ mm as a reference value, the peak load slightly increases by increasing the layer thickness, as shown with square dots in Fig.3(d). In the dynamic regime with, e.g., $v = 10$ m/s, this increase is much more pronounced, see Figs.3(b) and 3(d). By increasing $t$, the process zone size at the peak load is reduced, as shown in Figs.3(c).

## 4. Conclusions

In the present work, the inertia properties of finite thickness interfaces have been properly modeled by augmenting the classical interface element used for quasi-static analysis with a lumped mass matrix. Moreover, the parameters of the proposed CZM have been related to the adhesive thickness and to the adhesive Young modulus, quantities that can

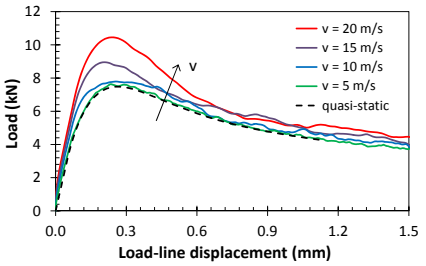


(a) Load vs. load-line displacement

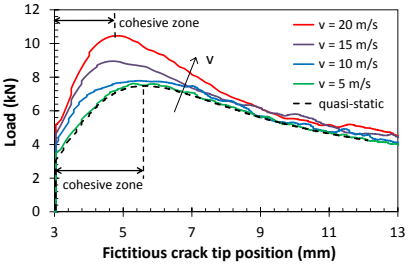


(b) Load vs. fictitious crack-tip position

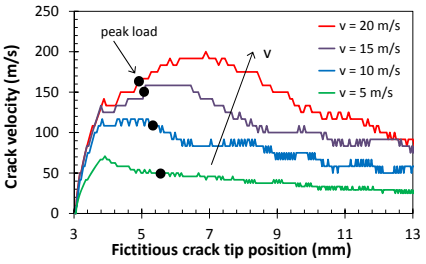


(c) Crack-tip velocity vs. fictitious crack-tip position

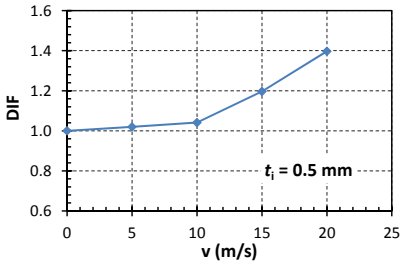


(d) DIF vs. velocity

Fig. 2. Effect of the load-line displacement velocity $v$, $t$ = 0.5 mm, $\rho$ = 2700 kg/m$^3$.

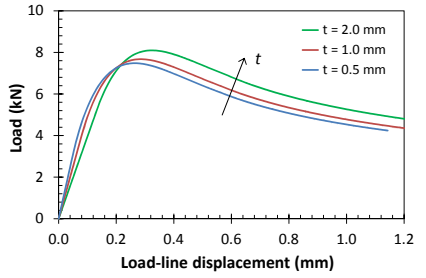


(a) Quasi-static

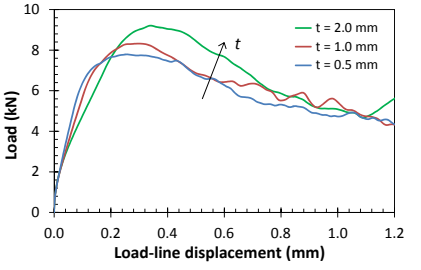


(b) Dynamic, $v$ = 10 m/s

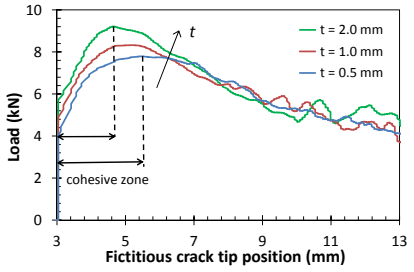


(c) Load vs. fictitious crack-tip pos. ($v$ = 10 m/s)

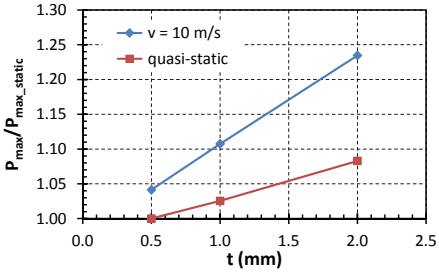


(d) Strength increase factor vs. adhesive thickness

Fig. 3. Effect of the adhesive thickness $t$ ($\rho$ = 2700 kg/m$^3$).

be ascertain with precision in composite materials testing. Examining a DCB test where the adhesive layer thickness is not negligible with respect to the other layers thickness, numerical results show that the interface stiffness and mass are important in the dynamic regime. Their effect regard both the dynamic strength increase factor, which is further increased as compared to the case when interface thickness effects are neglected, and the energy dissipated during the post-peak response.

## Acknowledgements

The research leading to these results has received funding from the European Research Council under the European Unions Seventh Framework Programme (FP/2007-2013) / ERC Grant Agreement n. 306622 (ERC Starting Grant Multi-field and multi-scale Computational Approach to Design and Durability of PhotoVoltaic Modules - CA2PVM). The support of the Italian Ministry of Education, University and Research to the project FIRB 2010 Future in Research Structural mechanics models for renewable energy applications (RBFR107AKG) is also gratefully acknowledged.

## References

Bertoldi, K., Bigoni, D., Drugan, J.W., 2007a. Structural interfaces in linear elasticity. Part I: nonlocality and gradient approximations. J. Mech. Phys. Solids, 55,1–34.

Bertoldi, K., Bigoni, D., Drugan, J.W., 2007b. Structural interfaces in linear elasticity. Part II: effective properties and neutrality. J. Mech. Phys. Solids, 55,35–63.

Bigoni, D., Movchan, A.B., 2002. Statics and dynamics of structural interfaces in elasticity. Int. J. Solids Struct., 39,4843–4865.

Brun, M., Guenneau, S., Movchan, A.B., Bigoni, D., 2010. Dynamics of structural interfaces: Filtering and focussing effects for elastic waves. J. Mech. Phys. Solids, 58, 1212–1224.

Camanho, P., Davila, C., 2002. Mixed-mode decohesion finite elements for the simulation of delamination growth in composite materials. NASA-TP-211401,1–19.

Carpinteri, A., Paggi, M., Zavarise, G., 2008. The effect of contact on the decohesion of laminated beams with multiple microcracks. Int. J. Solids Struct., 45,129–143.

Caverzan, A., Cadoni, E., Di Prisco, M., 2013. Dynamic tensile behaviour of high performance fibre reinforced cementitious composites after high temperature exposure. Mech. Mater., 59, 87–109.

Corigliano, A., Mariani, S., Pandolfi, A., 2006. Numerical analysis of rate-dependent dynamic composite delamination. Comp. Sci. Tech., 66, 767–775.

Elices, M., Guinea, G., Gmez, J., Planas, J., 2002. The cohesive zone model: Advantages, limitations and challenges. Engng. Fract. Mech.69, 137–163.

Li, S., Thouless, M.D., Waas, A.M., Schroeder, J.A., Zavattieri, P.D., 2005. Use of mode-I cohesive-zone models to describe the fracture of adhesively-bonded polymer-matrix composite. Comp. Sci. Tech., 65, 281–293.

Malvar, L.J., Ross, C.A., 1998. Review of strain rate effects for concrete in tension. ACI Mat. J., 95, 735-739.

Zhou, F., Molinari, J.F., Shioya, T., 2005. A rate-dependent cohesive model for simulating dynamic crack propagation in brittle materials. Engng. Fract. Mech., 72, 1383–1410.

Paggi, M., Wriggers, P., 2011a. A nonlocal cohesive zone model for finite thickness interfaces – Part I: mathematical formulation and validation with molecular dynamics. Comp. Mat. Sci. 50, 1625–1633.

Paggi, M., Wriggers, P., 2011b. A nonlocal cohesive zone model for finite thickness interfaces – Part II: FE implementation and application to polycrystalline materials. Comp. Mat. Sci. 50, 1634–1643.

Paggi, M., Wriggers, P., 2012. Stiffness and strength of hierarchical polycrystalline materials with imperfect interfaces. J. Mech. Phys. Solids 60, 557–572.

Spearot, D., Jacob, K., McDowell, D., 2004. Nonlocal separation constitutive laws for interfaces and their relation to nanoscale simulations. Mech. Mater. 36, 825–847.

Sumigawa, T., Hirakata, H., Takemura, M., Matsumoto, S., Suzuki, M., Kitamura, T., 2008. Disappearance of stress singularity at interface edge due to nanostructured thin film. Engng. Fract. Mech. 75, 3073–3083.

Tang, T., Hui, C.-Y., Glassmaker, N.J., 2005. Can a fibrillar interface be stronger and tougher than a non-fibrillar one? J. R. Soc. Interface 2, 505–516.

Wolf, D., Yamakov, V., Phillpot, S., Mukherjee, A., Gleiter, H., 2005. Deformation of nanocrystalline materials by molecular-dynamics simulation: relationship to experiments? Acta Mater. 53, 1–40.

Yamakov, V., Saether, E., Phillips, D.R., Glaessgen, E.H., 2006. Molecular-dynamics simulation-based cohesive zone representation of intergranular fracture processes in Aluminum. J. Mech. Phys. Solids 54,1899–1928.